Interlamination Insulation Design Considerations for Laminated Magnetics Operating at High Frequencies

Minsoo Kim and Mark G. Allen, *Fellow, IEEE*

Department of Electrical and Systems Engineering, University of Pennsylvania, Philadelphia, PA 19104 USA

A laminated magnetic core is comprised of alternating metallic magnetic layers and electrically insulating interlamination insulation layers, due to which eddy current losses in the core are suppressed. In practice, the nonzero conductivity of the interlamination insulation can lead to additional eddy current losses due to the electrical currents that travel across the layers. We present quantitative models which enable the determination of the necessary insulation quality of the interlamination insulation layers for various applications. For a given operating frequency range and given geometries/material properties of the magnetic material, the maximum tolerable conductivity of the interlamination material is calculated; this maximum is defined in such a way that the total eddy current losses, including the interlayer-induced losses, do not exceed the intrinsic material hysteresis losses. Understanding these maximum tolerable losses may open new design spaces for magnetic components; for example, allowing the use of interlamination insulation materials with finite conductivities may lead to a manufacturable, yet effective lamination approach for dc/dc converters based on integrated magnetics that can operate at RF switching frequencies (>3 MHz).

***Index Terms*—Eddy current loss, high frequency, interlamination insulation, laminated core design.**

NOMENCLATURE

Material Property:

r_{mp}	Conductivity ratio between the magnetic and insulation material.
δ_m [m]	Skin depth of the magnetic material.
$\mu_p\ (=\mu)$ [H/m]	Permeability of the insulation material.
μ_m [H/m]	Permeability of the magnetic material.
σ_m [S/m]	Conductivity of magnetic material.
σ_p [S/m]	Conductivity of interlamination insulation.

Homogenized Model Property:

r_{xy}	Conductivity anisotropy of the homogenized model.
δ_x [m]	Skin depth of the homogenized model.
μ_z [H/m]	Permeability of the homogenized model in z-axis.
σ_x [S/m]	Conductivity of the homogenized model in x-axis.
σ_y [S/m]	Conductivity of the homogenized model in y-axis.

Geometrical Property:

$i+1$	Number of magnetic layers.
i	Number of interlamination insulation layers.
N_d [turns/m]	Winding density.
t_m [m]	Thickness of an individual magnetic layer.
t_p [m]	Thickness of an individual insulation layer.
T [m]	Total thickness of the core.
w [m]	Width of the core.
γ	Fill factor.

Electrical Parameters:

B [T]	Magnetic flux density.
f [Hz]	Operating frequency.
I [A]	Magnetization current.
ϕ [$\mathrm{T \cdot m^2}$]	Total magnetic flux.
ϕ_0 [$\mathrm{T \cdot m^2}$]	Total magnetic flux assuming no demagnetization.
ω [rad/s]	Angular frequency.

Ratios:

ETH $(=(P_{e,d}+P_{e,i})/P_h)$	The ratio of the total eddy current loss to the total hysteresis loss.
$k(=w/\delta_x)$	The ratio of the core width to the skin depth of the homogenized model.
$k_m(=t_m/\delta_m)$	The ratio of the magnetic layer thickness to the skin depth of the magnetic material.
$l(=T\gamma/\delta_m)$	The ratio of the total magnetic material thickness to the skin depth of the magnetic material.
$r_{\mathrm{mp}}(=\sigma_m/\sigma_p)$	Material conductivity ratio of the magnetic material to the interlamination insulation material.
$r_{xy}(=\sigma_x/\sigma_y)$	Conductivity anisotropy of the homogenized model.

I. INTRODUCTION

EMERGING needs for magnetic materials that can operate at high frequencies (>3 MHz) in power electronics applications have motivated further developments in the design and

Manuscript received July 13, 2018; revised December 18, 2018; accepted March 20, 2019. Date of publication June 18, 2019; date of current version July 18, 2019. Corresponding author: M. G. Allen (e-mail: mallen@upenn.edu).

Color versions of one or more of the figures in this paper are available online at http://ieeexplore.ieee.org.

Digital Object Identifier 10.1109/TMAG.2019.2910477

fabrication of laminated magnetic cores [1]–[3]. For example, switched-mode dc/dc converters and transformers, that are ubiquitous in power electronics, could be further miniaturized if typical ferrite-based inductive devices are replaced by metallic laminated cores with higher saturation flux densities [4].

Typically, a laminated magnetic core is comprised of a desired number of layers of electrically insulated, thin soft magnetic alloy, in which the layer thicknesses are smaller than the skin depth of the magnetic material at desired operating frequencies. If the magnetic layers are metallic and relatively highly conducting, and the operating frequencies are high, the maximum layer thicknesses can become quite small. When neighboring magnetic layers are electrically isolated from each other by perfectly insulating interlamination layers, any eddy currents are ideally completely confined within the thin magnetic layers. At frequencies where displacement currents in the core can be neglected, there are no eddy currents that are traveling between the magnetic layers. In this case, the total eddy current loss of the core is the sum of the intralayer eddy current losses generated within the individual magnetic layers. The areal magnetic energy storage capacity of the perfect laminated core can be scaled up by increasing the number of magnetic layers while the intralayer losses are suppressed to a desired level, such as the level of material hysteresis losses. If the interlayer insulation material has nonzero conductivity, eddy current losses within the lamination stack may increase due to the changing profiles of eddy currents which are enabled by leakage of current through the interlayer insulation.

The thicknesses of the individual magnetic layers of a MHz metallic-laminated core are typically limited to a few micrometers, or less, due to the small skin depths of the magnetic materials at these frequencies. To achieve a laminated magnetic core in which a high percentage of the volume of the core comprises magnetic material (i.e., high fill-factor), interlamination layers with even smaller thicknesses than the magnetic layers are preferred. A desirable laminated core manufacturing technology should combine excellent scalability (i.e., the ability to achieve thick cores, which implies many thin, stacked layers) with the ability to achieve controlled, microscale, or nanoscale individual layer thicknesses. Traditional lamination processes, typically based on milling, stacking, and/or cutting, will likely have more difficulty in achieving the desired thicknesses than deposition-based lamination approaches.

Physical vapor deposition has been employed to create laminated magnetic cores; the deposition of alternating metallic magnetic layers and highly resistive oxide-based interlamination layers has been realized [5], [6]. Such oxide interlamination materials are sufficiently resistive to suppress interlayer conduction even at very high frequencies (>30 MHz). However, the relatively high production costs of vacuum processes and the technical difficulties in achieving thick cores comprising many layers (i.e., slow deposition rate and high built-in stress) are challenges for this approach to achieve high-power devices.

Electrodeposition has also been employed to create laminated magnetic cores; thick cores with large volumes of magnetic material can be realized due to the superior scalability (i.e., high deposition rate and lower stress) of this process. However, the continuous deposition of multiple magnetic layers is feasible only at the expense of using conductive interlamination materials. Hence, electrodeposition-based approaches may involve additional interlamination insulation processes (i.e., deposition/removal of sacrificial material [4], [7], [8], or SU-8 patterning [9], [10]) during or after the lamination process; these ancillary steps may add fabrication complexities.

Using an interlamination insulation material with an intermediate range of electrical conductivity may lead to a manufacturable lamination process while simultaneously suppressing the total eddy current losses to acceptable levels. In such cases, a continuous, sequential electrochemical deposition of alternating magnetic and interlamination layers could be a potential manufacturing approach, if the chosen interlamination material is sufficiently conductive to allow the electrochemical deposition of the magnetic material while also being sufficiently resistive to suppress the eddy currents to a tolerable level. Designing a proper interlamination insulation for this fabrication approach necessitates a comprehensive core loss model that considers both eddy and hysteresis losses.

We consider a theoretical model (i.e., Bewley model) that assumes a "leaky" laminated core as a homogeneous material with finite anisotropic conductivity [10]. This model was previously utilized to analyze the effect of "edge burrs," i.e., the electrical shorts that are formed during core singulation [10], [11] for electric motors; however, in this model, intralayer lamination losses were neglected. The total eddy current losses were treated as a superposition of intralayer losses assuming interlayer conductivity of zero, with the Bewley model assuming zero intralayer eddy current losses in [12]. In this paper, we codify these models with an eye toward their application in high-frequency magnetics. By extrapolating the previous analytical studies, we estimate necessary interlamination insulation quality as a function of operating frequency, core geometry, and the magnetic/electrical properties of the lamination materials, such that the total eddy current loss including losses induced by nonzero interlayer conductivity is tolerable (i.e., does not exceed the intrinsic material hysteresis losses). Based on the study, we present an interlamination insulation design example for laminated cores operating at high frequencies (beyond the MHz range).

II. Quantification of Necessary Interlamination Insulation Quality

A. Calculation Procedure

We calculate the constraints on the necessary interlamination insulation quality in three steps. First, we calculate the total eddy current losses and hysteresis losses of a laminated core based on theoretical models. The homogenized model is considered in which a laminated core is modeled as a homogeneous material with finite anisotropic conductivity. In this model, the losses generated within the individual magnetic layers (i.e., intralayer eddy current losses) are neglected; these losses will later be superposed with the losses predicted by this homogenized model. The losses calculated from this model represent the eddy current losses from the "delocalized"

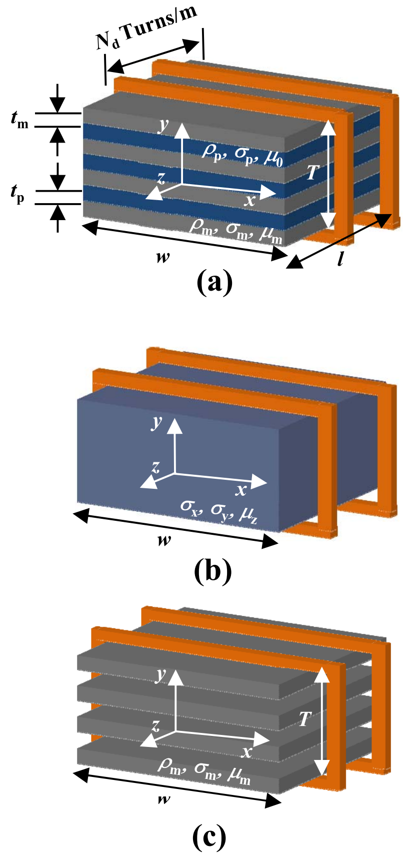

Fig. 1. (a) Schematic of a laminated core. A core comprises alternating magnetic layers (permeability of μ_m and conductivity of σ_m) and interlayer lamination layers (μ_0, σ_p). (b) Homogenized model of the laminated core. In this model, the core is considered as a single material with anisotropic conductivity. The conductivity of the model along x- and y-axes are σ_x and σ_y, respectively. (c) Discrete layer model of the laminated core. The interlamination insulation conductivity is zero. Complete electrical insulation between each layer is assumed.

currents that are flowing among multiple magnetic layers due to finite interlamination conductivities. This loss is referred to as the delocalized eddy current losses.

The intralayer eddy current losses are calculated based on a discrete layer model where electrically isolated individual magnetic layers are assumed [see Fig. 1(c)]. The total eddy current loss within a laminated core is the superposition of the intralayer eddy current losses and the delocalized eddy current losses calculated from the homogenized model. The calculation of the hysteresis losses is performed based on a parallelogram model, in which parallelogram-shaped hysteresis loops are assumed [13]. Next, we calculate the ratio of the total eddy current loss to the total hysteresis loss (ETH). The frequency at which the ETH exceeds unity is defined as the cutoff frequency f_c. This frequency is the higher bound of the operating frequency range. In other words, the total eddy current loss is defined to be tolerable up to the frequency where it is comparable to the ETH. Beyond this frequency, the eddy current losses will dominate over the hysteresis losses, since the eddy losses increase in proportion to $f^{1.5} - f^2$, while the hysteresis losses increase in proportion to $f - f^{1.5}$ [14]. Defining the operating frequency to be equal to the cutoff frequency, in turn defines the minimum tolerable conductivity ratio between the magnetic and interlayer insulation materials ($r_{\min,\mathrm{mp}}$) at the operating frequency of interest. Third, the $r_{\min,\mathrm{mp}}$ is converted into the maximum tolerable conductivity of the interlayer insulation ($\sigma_{\max,p}$), which represents the necessary interlamination insulation quality.

B. Delocalized Eddy Current Losses

Fig. 1(a) shows a laminated core comprising $i+1$ layers of magnetic material and i layers of interlayer material, where t_m and t_p are the thicknesses of an individual magnetic layer and an individual interlamination layer, respectively. The symbols for the geometrical parameters [e.g., the individual thicknesses of magnetic/interlamination insulation layers (t_m, t_p), core width (w), and total core thickness (T)] and the material properties (i.e., conductivity, resistivity, and permeability) are presented in Nomenclature and Fig. 1. Note that we assume linear magnetic materials with constant magnetic permeabilities.

The delocalized eddy current loss of the laminated core is calculated based on the homogenized model [see Fig. 1(b)]. The conductivity along the y-axis of the model, which is calculated based on the summation of the resistances of the individual magnetic and interlamination layers, is

$$\sigma_y \approx \sigma_p \cdot \left(\frac{1}{1-\gamma}\right) \tag{1}$$

where the fill factor γ is

$$\gamma = \frac{(i+1)t_m}{T}. \tag{2}$$

Similarly, the conductivity along the x-axis of the model is calculated based on the summation of the conductances of the individual layers

$$\sigma_x \approx \sigma_m \gamma. \tag{3}$$

The conductivity anisotropy of the homogenized model is $r_{xy} = \sigma_x/\sigma_y$. Equations (1) and (3) are accurate for laminated cores with fill factors smaller than 0.95 and r_{mp} (i.e., the material conductivity ratio between the magnetic material and the interlamination insulation material, σ_m/σ_p) larger than 1000 (see the Appendix). The permeability of the homogenized model along the z-axis is

$$\mu_z \approx \mu_m \gamma. \tag{4}$$

Assuming that the core is wrapped with a wire (winding density $= N_d$ [turns/m]) within which a sinusoidal magnetizing current I is induced, subjecting the core to a unidirectional magnetic field with negligible magnetic flux leakage, the governing equation for the resultant magnetic field is

$$\frac{\partial^2 H_z}{\partial x^2} + \frac{1}{r_{xy}}\frac{\partial^2 H_z}{\partial y^2} = \left(\frac{1+j}{\delta x}\right)^2 H_z \tag{5}$$

where

$$\delta x = \sqrt{\frac{r_{xy}}{\pi f \mu_z \sigma_x}}. \tag{6}$$

Note that I and H_z are the phasor representation of the peak current and the induced magnetic field intensity along the z-axis, respectively. The corresponding magnetic flux (ϕ) and electromotive forces (EMFs) are also the peak values that are represented by phasors; on the contrary, the calculated eddy and hysteresis power losses and stored magnetic energies that are presented elsewhere are average values. The skin depth of the homogenized model (δ_x) is a measure of the magnetic flux diffusion depth at an operating frequency f. We use the subscript x for this skin depth, since our subject of interest is to assess the magnetic field diffusion in the x-direction at an operating frequency. The boundary condition is

$$H_z = H_0 = N_d I \tag{7}$$

at $(x, y) = (\pm 0.5w, 0)$ and $(x, y) = (0, \pm 0.5T)$. The corresponding magnetic flux assuming no eddy current losses within the core (ϕ_0 [$\mathrm{T} \cdot \mathrm{m}^2$]) is

$$\phi_0 = \mu_z H_0 w T. \tag{8}$$

The exact solution of the normalized magnetic flux (ϕ/ϕ_0) is presented in [10]. The normalized magnetic flux can be expressed as a function of k and l such as

$$\frac{\phi}{\phi_0} = \frac{\tanh\left\{\left(\frac{1+j}{2}\right)k\right\}}{\left(\frac{1+j}{2}\right)k} + \frac{8}{\pi^2}\sum_{n=1,3,5\ldots}^{\infty}\frac{1}{n^2}\left(\frac{1}{1-j\frac{n^2\pi^2}{2k^2}}\right) \times \left[\frac{\tanh\left(\frac{l}{\sqrt{2}}\sqrt{\frac{n^2\pi^2}{k^2}+j}\right)}{\frac{l}{\sqrt{2}}\sqrt{\frac{n^2\pi^2}{k^2}+j}}\right] \tag{9}$$

where k and l are

$$k = \frac{w}{\delta_x} \quad \text{and} \quad l = \frac{T\gamma}{\delta_m}. \tag{10}$$

The parameter k represents the ratio of the core width to the skin depth of the homogenized model, while l represents the ratio of the total magnetic material thickness to the skin depth of the magnetic material. The solution (9) can be simplified based on two assumptions. First, when r_{xy} is very large, the boundary conditions imposed by the top and bottom of the laminated core can be neglected (i.e., negligible end effect). Then, (5) is reduced to the 1-D ordinary differential equation

$$\frac{d^2 H_z}{dx^2} = \left(\frac{1+j}{\delta_x}\right)^2 H_z. \tag{11}$$

From (11), we can conclude that the directions of the eddy currents will be limited to the $\pm y$ directions. The normalized flux simplifies to

$$\frac{\phi}{\phi_0} = \frac{\tanh\left\{\frac{k(1+j)}{2}\right\}}{\frac{k(1+j)}{2}}. \tag{12}$$

If we further assume that the demagnetization within the core is negligible, the H_z term on the right-hand side of (11) can be substituted by H_0 to yield

$$\frac{d^2 H_z}{dx^2} = \left(\frac{1+j}{\delta_x}\right)^2 H_0. \tag{13}$$

These assumptions will be validated in the Appendix. The solution to this equation is

$$\frac{\phi}{\phi_0} = 1 - \frac{jk^2}{6} = 1 - \frac{j\omega\mu_z\sigma_y w^2}{12}. \tag{14}$$

The EMF resulting from a unit length of the core (EMF[V/m]) is

$$\mathrm{EMF} = -j\omega\phi N_d \tag{15}$$

where ω[rad/s] is the angular frequency. The real part of the EMF is responsible for the delocalized eddy current loss. The power loss due to the delocalized eddy current per length of the core ($P_{e,d}$[W/m]) is

$$P_{e,d} = \frac{1}{2}I|\mathrm{Re}(\mathrm{EMF})| = \frac{\omega\phi_0 H_0}{2}\left|\mathrm{Im}\left(\frac{\phi}{\phi_0}\right)\right| = \frac{(\omega\phi_0)^2 w\sigma_y}{24T}. \tag{16}$$

C. Intralayer Eddy Current Losses

The intralayer eddy current loss of the laminated core is calculated based on the discrete layer model [see Fig. 1(c)]. Since the interlayer conduction is neglected, the total intralayer loss is calculated by multiplying the number of the magnetic layers, $i+1$, and the eddy current loss generated from a single magnetic layer. The loss from a single layer can be calculated from the following governing equation [15], [16]:

$$\frac{d^2 H_z}{dy^2} = \left(\frac{1+j}{\delta_m}\right)^2 H_0 \tag{17}$$

where δ_m is the well-known skin depth of the magnetic material

$$\delta_m = \sqrt{\frac{1}{\pi f \mu_m \sigma_m}}. \tag{18}$$

Note that (17) can be derived from (5) after substituting $r_{xy} = 1$, assuming negligible demagnetization within the magnetic layer, and neglecting d^2H_z/dx^2 (i.e., neglecting the end effect, which is usually acceptable since w is typically much larger than t_m). The H_0 is identical to (7); hence, the corresponding flux assuming no eddy current losses within the single layer ($\phi_{0,\mathrm{single}}$ [$\mathrm{T} \cdot \mathrm{m}^2$]) is

$$\phi_{0,\mathrm{single}} = \mu_m H_0 w t_m. \tag{19}$$

Solving (17) leads to

$$\frac{\phi}{\phi_{0,\mathrm{single}}} = 1 - \frac{jk_m^2}{6} = 1 - \frac{jt_m^2}{6\delta_m^2} = 1 - \frac{j\omega\mu_m\sigma_m t_m^2}{12} \tag{20}$$

where $k_m = t_m/\delta_m$.

The intralayer eddy current loss of a single layer ($P_{e,i,\mathrm{single}}$) is

$$P_{e,i,\mathrm{single}} = \frac{\sigma_m t_m(\omega\phi_{0,\mathrm{single}})^2}{24w}. \tag{21}$$

Since $\phi_{0,\mathrm{single}}$ is $\phi_0/(i+1)$, $P_{e,i,\mathrm{single}}$ is

$$P_{e,i,\mathrm{single}} = \frac{\sigma_m t_m(\omega\phi_0)^2}{24w(i+1)^2}. \tag{22}$$

Hence,

$$P_{e,i} = (i+1)P_{e,i,\mathrm{single}} = \frac{\sigma_m t_m(\omega\phi_0)^2}{24w(i+1)}. \tag{23}$$

D. Hysteresis Losses

The hysteresis energy loss per core length and per magnetization cycle ($W_{h,\mathrm{cycle}}$ [J/m]) can be calculated as a function

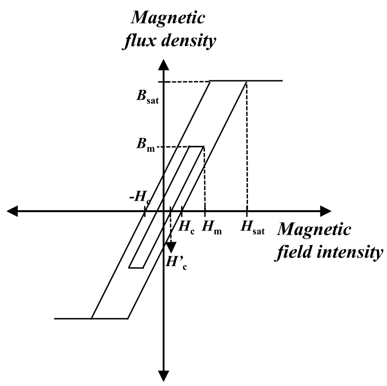

Fig. 2. Parallelogram model for a magnetic material hysteresis loop. The major loop is formed when the induced magnetic field density is H_{sat} and the corresponding saturation flux density is B_{sat}. The minor loops, which are self-similar to the major loop, are formed when the induced magnetic field intensity H and corresponding B vary between H_{sat} and B_{sat}.

of the induced magnetic field ($H(x, y)$), magnetic flux density ($B(x, y)$) and the arbitrary shape factor, S [14]

$$W_{h,\text{cycle}} = \int\int 2SBH\,dx\,dy \tag{24}$$

The hysteresis power loss per length of the core (P_h [W/m]) is

$$P_h = fW_{h,\text{cycle}}. \tag{25}$$

The parameter S is defined by the mathematical model of the hysteresis loop. For simplicity, we model the geometry of the hysteresis loop as a parallelogram [13], in which B_{sat}, H_{sat}, and the coercivity, H_c are defined as in Fig. 2. Using this model simplifies the hysteresis loss comparison between various alloys and leads to a simple, closed ETH formula. We assume that all the minor loops, i.e., the loops that are generated by the excitation smaller than H_{sat}, are geometrically similar to the major loop, i.e., the loop that is generated by the excitation identical to/or larger than H_{sat}. From the calculated area of the loop, $W_{h,\text{cycle}}$ is

$$W_{h,\text{cycle}} = \int\int 4BH_c'\,dx\,dy. \tag{26}$$

Comparing (24) and (26) yields

$$S = \frac{2H_c'}{H} = \frac{2H_c}{H_{\text{sat}}}. \tag{27}$$

Note the parameter S can be defined as a constant in our parallelogram model; however, in general, an appropriate polynomial S could be defined to model the curvature of a hysteresis loop with higher accuracy as depicted in [13]. In the parallelogram model, the parameter S quantifies the "degree" of hysteresis; the materials with larger S dissipate more energy via hysteresis per given input magnetic energy. When the single permeability μ is defined between H and B ($B = \mu_z H$) and the demagnetization within the magnetic material is assumed to be negligible ($H = H_0$, $B = B_0$), P_h is

$$P_h = \frac{2fS\phi_0^2}{\mu_z wT}. \tag{28}$$

E. Loss Ratios

The delocalized eddy current loss to hysteresis loss ratio ($P_{e,d}/P_h$) is

$$\frac{P_{e,d}}{P_h} = \frac{\pi w^2}{12S\delta_x^2} = \frac{\pi k^2}{12S}. \tag{29}$$

Similarly, the total intralayer eddy current loss to hysteresis loss ratio ($P_{e,i}/P_h$) is

$$\frac{P_{e,i}}{P_h} = \frac{\pi t_m^2}{12S\delta_m^2} = \frac{\pi k_m^2}{12S}. \tag{30}$$

The $P_{e,d}/P_h$ and $P_{e,i}/P_h$ of representative metallic magnetic materials are plotted in Fig. 3. The total eddy current loss to the ETH of the laminated core is

$$\text{ETH} = \frac{P_{e,d} + P_{e,i}}{P_h} = \frac{\pi}{12S}\left[\left(\frac{w}{\delta_x}\right)^2 + \left(\frac{t_m}{\delta_m}\right)^2\right]. \tag{31}$$

The first and the second terms of (31) represent $P_{e,d}/P_h$ and $P_{e,i}/P_h$, respectively. When the core geometries and operating frequencies are fixed, the loss ratio ETH will be dominated by $P_{e,i}$ as r_{xy} increases (since δ_x increases, and thereby $P_{e,d}$ decreases while $P_{e,i}/P_h$ is fixed). When r_{xy} is infinite (interlamination material conductivity being zero), the loss calculated from the discrete layer loss model ($P_{e,i}$) will be sufficient to predict the total eddy current loss. On the other hand, if r_{xy} is small (but still larger than $\sim$1000 not to violate the assumptions of the homogenized model), the delocalized eddy current losses, $P_{e,d}$, may dominate the total eddy current loss.

From (29) and (30), the intralayer eddy current loss to delocalized eddy current loss ratio is

$$\frac{P_{e,d}}{P_{e,i}} = \frac{w^2}{r_{\text{mp}}t_m^2}\left(\frac{\gamma}{1-\gamma}\right) = \frac{w^2}{w_c^2} \tag{32}$$

where w_c which is referred to as the critical width is

$$w_c = t_m\sqrt{\frac{r_{\text{mp}}(1-\gamma)}{\gamma}}. \tag{33}$$

The ratio ETH can be expressed as (34). Note the delocalized eddy current losses and the intralayer eddy current losses are identical when $w_c/w = 1$

$$\text{ETH} = \frac{P_{e,d} + P_{e,i}}{P_h} = \frac{P_{e,d}}{P_h}\left(1 + \frac{P_{e,i}}{P_{e,d}}\right) = \frac{\pi k^2}{12S}\left(1 + \frac{w_c^2}{w^2}\right). \tag{34}$$

F. Cutoff Frequency Analysis

The cutoff frequency of the laminated core (f_c) is defined when ETH equals unity. From (31), it can be shown that

$$f_c = \left[\frac{12Sr_{\text{mp}}}{\pi^2\mu_m\sigma_m\left(w^2 + w_c^2\right)}\right]\left(\frac{1-\gamma}{\gamma}\right). \tag{35}$$

This can be also expressed as

$$f_c = \left(\frac{1}{1 + \frac{w_c^2}{w^2}}\right)f_{c,\text{homo}} \tag{36}$$

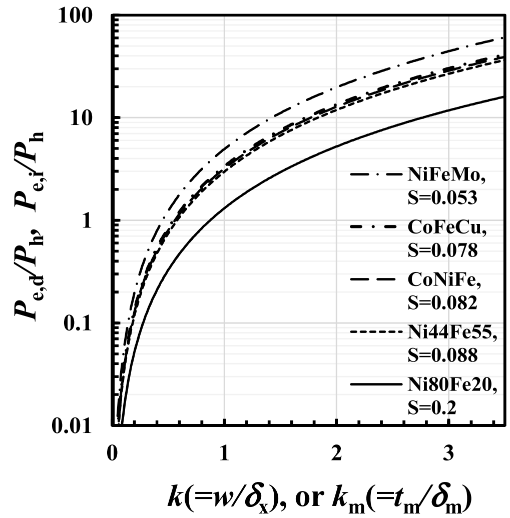

Fig. 3. Ratio of the delocalized eddy current loss to the hysteresis loss ($P_{e,d}/P_h$) as a function of the ratio of the core width to the skin depth of the homogenized model ($k = w/\delta_x$); or the ratio of the intralayer eddy current loss to the hysteresis loss ($P_{e,i}/P_h$) as a function of the ratio of the individual magnetic layer thickness to the skin depth of the magnetic material ($k_m = t_m/\delta_m$). The shape factors (S) of the respective materials are calculated from the actual hysteresis loops [4], [17]–[20]; however, these values could vary depending on various parameters, such as microscopic material structure (e.g., thickness-dependent grain sizes and crystallinity) and core geometry (e.g., shape anisotropy).

where $f_{c,\text{homo}}$ is

$$f_{c,\text{homo}} = \left(\frac{12S}{\pi}\right)\left(\frac{r_{\text{mp}}}{\pi\,\mu_m\sigma_m w^2}\right)\left(\frac{1-\gamma}{\gamma}\right). \tag{37}$$

$f_{c,\text{homo}}$ is referred to as the cutoff frequency of the homogenized model, since this can also be calculated from $P_{e,d}/P_h = 1$, assuming zero intralayer eddy current losses. Hence, when the condition $w \gg w_c$ is satisfied

$$f_c \approx f_{c,\text{homo}} \quad (w \gg w_c). \tag{38}$$

On the other hand, if the condition $w \ll w_c$ is satisfied, then

$$f_c \approx f_{c,\text{disc}} \quad (w \ll w_c) \tag{39}$$

where, $f_{c,\text{disc}}$, defined as the cutoff frequency of the discrete layer model is

$$f_{c,\text{disc}} = \left(\frac{12S}{\pi}\right)\left(\frac{1}{\pi\,\mu_m\sigma_m t_m^2}\right). \tag{40}$$

Analogous to $f_{c,\text{homo}}$, this cutoff frequency, $f_{c,\text{disc}}$, can be calculated from $P_{e,i}/P_h = 1$ assuming zero delocalized eddy current losses. The $f_{c,\text{homo}}$ and $f_{c,\text{disc}}$ are asymptotes of f_c; the intersection between $f_{c,\text{homo}}$ and $f_{c,\text{disc}}$ is formed at $w = w_c$. For the representative soft magnetic metallic alloys presented in Fig. 3, we may assume a nominal shape factor, $S = 0.1$ (i.e., the average of the calculated S for the alloys shown in Fig. 3). Equation (35) is a function of the material properties that are intrinsic to the desired magnetic material (i.e., μ_m, σ_m, and S), fill factor (γ), core geometries (i.e., w and t_m), and the conductivity ratio between the magnetic and insulation materials (r_{mp}). In a laminated core design process, the former two are mainly determined by the desired magnetic energy storage density of a laminated core, while the latter two are determined by analyzing (35) within an appropriate parametric space as will be detailed shortly.

TABLE I

Fixed Magnetic Core Parameters

f [MHz]	10
Power handling [W]	1
μ_m [H/m]	$100\mu_0$
σ_m [S/m]	10^7
S (Shape factor)	0.1

Once the material properties and the geometries of the magnetic layers are fixed, the material conductivity ratio r_{mp} can be determined such that the cutoff frequency (f_c) of the laminated core is identical to, or higher than the desired operating frequency (f). The minimum tolerable material conductivity ratio, $r_{\text{min,mp}}$, is defined when f_c is equal to f

$$r_{\text{min,mp}} = \left(\frac{\pi^2\mu_m\sigma_m w^2 f}{12S - \pi^2\mu_m\sigma_m t_m^2 f}\right)\left(\frac{\gamma}{1-\gamma}\right). \tag{41}$$

When the conductivity of the magnetic material (σ_m) is determined, the maximum tolerable conductivity of the interlayer insulation ($\sigma_{\text{max},p}$) can be calculated using

$$\sigma_{\text{max},p} = \frac{\sigma_m}{r_{\text{min,mp}}}. \tag{42}$$

Note that (35)–(42) are derived from a definition of f_c which is based on the criterion, ETH $= 1$. However, this criterion can be modified depending on the desired balance between core lamination fabrication cost and core performance; for example, one may tolerate smaller eddy current losses (by defining f_c where ETH < 1) if the fabrication cost for the realization of the laminated cores with thinner laminations is acceptable.

III. Interlamination Insulation Design Example For High-Frequency Laminated Cores

We illustrate the utility of the presented analysis by designing an interlamination insulation for a high-frequency laminated magnetic core. Applications for such a core may include miniaturized inductive devices for compact dc/dc power conversion. Design constraints are made such that the laminated cores with proper interlamination insulation would be able to process a desired level of power within a minimized form factor, smaller than that of a typical ferrite core.

Suppose a laminated permalloy ($Ni_{80}Fe_{20}$) magnetic core with μ_m of $100\mu_0$ is designed to process 1 W within an inductor operating at 10 MHz (Table I). Assume that this permeability can be always achieved by employing an appropriately patterned air gap within the core material. First, the necessary volume and the overall geometry of the core are estimated from the power handling constraints. Second, the individual magnetic layer thicknesses, core widths, and the conductivity ratios between magnetic and insulation materials are determined based on a cutoff frequency analysis. Finally, the necessary interlamination insulation quality of the core is determined.

A. Fill Factor

What would be the relevant range of the fill factor? We define the averaged saturation flux density of a laminated core ($B_{\text{sat,lam}}$) as the product of the saturation flux density of the magnetic material ($B_{\text{sat},m}$) and the lamination fill factor (γ)

$$B_{\text{sat,lam}} = \gamma\, B_{\text{sat},m}. \tag{43}$$

Note that one of the main reasons to prefer laminated soft magnetic cores to typical ferrite materials is the superior saturation flux densities of metallic alloys; hence, we may define a minimum lamination fill factor where the difference between $B_{\text{sat,lam}}$ and $B_{\text{sat},m}$ of typical ferrites is marginal. Since $B_{\text{sat},m}$ of permalloy is approximately 1 T while those of ferrites are 0.3-0.5 T [21], 50% could be regarded as the minimum fill factor. On the other hand, the maximum achievable lamination fill factor is defined by the limitation of a particular interlamination insulation deposition process; this may vary depending on how conformal and uniform a deposition can be achieved through different deposition approaches. A high fill factor of 95% can be achieved based on sputtering since nanoscale thick (<50 nm) interlamination insulation layers can be realized; this would be a reasonable approximation of the maximum fill factor [22].

B. Core Width and Total Core Thickness

Assume that the laminated permalloy core is operating at a reasonably high flux to demonstrate higher energy density compared with ferrites (i.e., $B_0 = 0.3$ T, which is close to the saturation of typical ferrites, yet smaller than $B_{\text{sat,lam}}$ of a 50% fill-factor permalloy core, 0.5 T). The volumetric energy density (E [J/m^3]) of the core is

$$E = \frac{B_0^2}{2\mu_z} = 358\ [\text{J/m}^3]. \tag{44}$$

The core must store 0.1 μJ per cycle (since operating frequency $(f) = 10$ MHz), within its volume $V = AT$, where A is the projected area of the core

$$E = 358\ [\text{J/m}^3] = \frac{10^{-7}\ [\text{J}]}{AT[\text{m}^3]}. \tag{45}$$

Thick laminated magnetic cores with their total thicknesses (T) exceeding 50 μm have been demonstrated based on electrodeposition-based approaches [4], [19]. If this is achieved, then the necessary footprint area of the core would be on the order of a few square millimeters ($A < 5.6$ mm^2). The relevant core width could range between a few hundreds of micrometers to a few millimeters depending on the choice of inductor geometries (e.g., racetrack, toroid, and stripline [3]).

C. Cutoff Frequency Analysis Case 1: Laminated Core With 50% Fill Factor

Fig. 4 presents cutoff frequency, f_c (solid lines), that are parameterized by r_{mp}, as a function of the core width, w; the calculation of f_c is based on (35). The shaded region

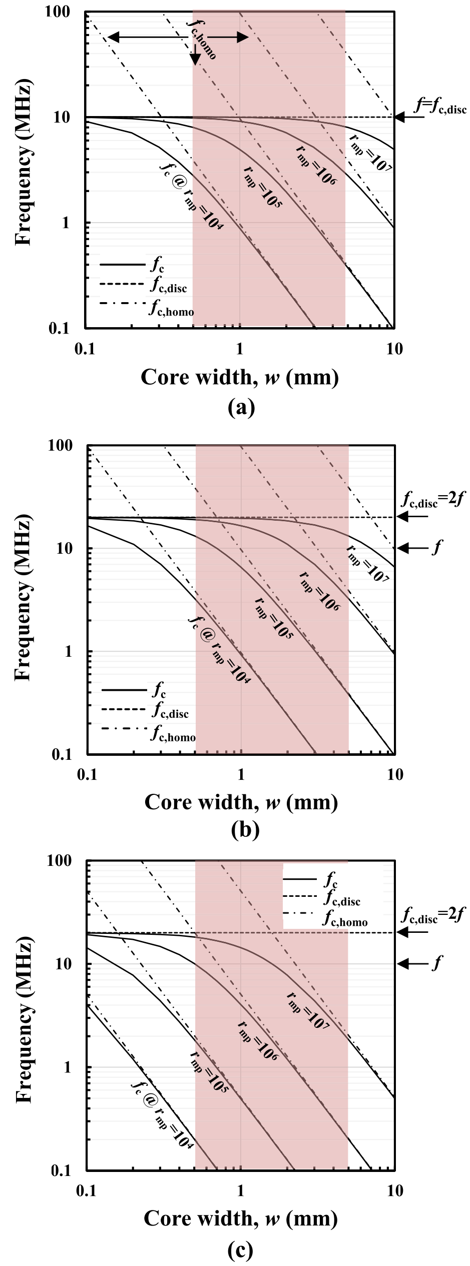

Fig. 4. Cutoff frequency (solid line) as a function of core width (w), parameterized by the material conductivity ratio (r_m). The shaded region (500 μm < w < 5 mm) represents the potential range of the core width. The frequencies are calculated for the following cases. (a) 50% fill factor and $t_m = 3.1$ μm. (b) 50% fill factor and $t_m = 2.2$ μm. (3) 95% fill factor and $t_m = 2.2$ μm. The dotted horizontal lines represent the cutoff frequencies of the discrete layer model ($f_{c,\text{disc}}$), while the dotted diagonal lines represent the cutoff frequencies of the homogenized model ($f_{c,\text{homo}}$).

(500 μm < w < 5 mm) corresponds to the potential range of the core width that was discussed in Section III-B. Based on the cutoff frequency analysis, proper individual magnetic layer thicknesses, core widths, and tolerable insulation conductivities are designed for the laminated cores with extreme fill factors, 50% or 95%; we will first consider $\gamma = 50\%$.

The cutoff frequency analysis begins from the fact that, by definition, the operating frequency cannot be larger than the cutoff frequency, where the sum of intra- and delocalized eddy current losses is equal to the ETH. Hence

$$f \le f_c < f_{c,\text{disc}}. \tag{46}$$

The choice of t_m depends on how the total tolerable eddy current loss would be allocated between the intra- and delocalized eddy current losses. From (40) and (46), the acceptable range of t_m can be back calculated as

$$t_m < t_{m,c} = \sqrt{\frac{12S}{\pi^2 \mu_m \sigma_m f}} \tag{47}$$

when the critical magnetic layer thickness, $t_{m,c}$ (3.1 μm at 10 MHz), is the magnetic layer thickness that makes $f_{c,\text{disc}}$ identical to the desired operating frequency (f). Choosing $t_m = t_{m,c} = 3.1$ μm means that only the intralayer eddy current losses will be tolerated without accepting any delocalized eddy current losses. From Fig. 4(a), we observe that the cores with all ranges of w fail to operate at 10 MHz regardless of r_{mp}, due to the non-zero delocalized eddy currents, although a higher r_{mp} results in a higher f_c at a given w.

To operate a core at a desired frequency while accommodating non-zero delocalized eddy current losses, a smaller t_m that will lead to an $f_{c,\text{disc}}$ significantly higher than the desired operating frequency (or, in other words, a smaller t_m that will lead to a smaller intralayer eddy current losses) would be an appropriate choice. For example, consider

$$t_m = \frac{t_{m,c}}{\sqrt{2}} \tag{48}$$

(i.e., $t_m = 2.2$ μm, in this case) which will lead to $f = 2f_{c,\text{disc}}$ (=20 MHz) [see Fig. 4(b)]. The corresponding critical width (w_c, where $f_{c,\text{disc}} = f_{c,\text{homo}}$) conveniently becomes the maximum allowable core width, smaller than which the laminated core would operate at the desired operating frequency [i.e., satisfying (46), $f = 10$ MHz $\le f_c$]. At $w = w_c$, $P_{e,d}/P_{e,i}$ is unity; the total tolerable eddy current loss is equally distributed to intra- and delocalized eddy current losses.

After t_m is defined, the appropriateness of a specific r_{mp} can be easily determined by evaluating whether the desired width of the laminated core is smaller than w_c. For an example, laminated cores with $r_{\text{mp}} = 10^7$ will operate at 10 MHz regardless of their core widths (0.5 mm $< w < w_c \approx 7$ mm). The cores with $r_{\text{mp}} = 10^6$ will operate at 10 MHz if the cores are smaller than $w_c \approx 2.1$ mm. The fact that w is limited to w_c implies that the total thickness of the core should exceed a certain extent, since the desired volume of the magnetic material is fixed by power handling constraints. Although thicker cores with smaller widths exhibit less delocalized eddy current losses compared with their counterparts (with smaller total thicknesses and larger widths), the achievable total thickness of the core could be limited due to fabrication constraints. In this case, a laminated magnetic core may rather be comprised of a group of electrically isolated "subcores" of which individual widths are smaller than the critical widths as depicted in Fig. 5. The gap between the subcores should be designed such that the subcores are electrically isolated while the decrease of the fill factor due to the presence of the gap is minimized.

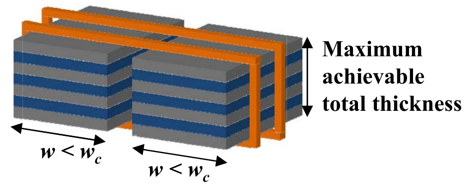

Fig. 5. Laminated core comprised of two isolated subcores.

D. Cutoff Frequency Analysis Case 2: Laminated Core With 95% Fill Factor

A similar analysis can be performed for laminated cores with 95% fill factor [see Fig. 4(c)]. The laminated cores with millimeter-scale widths will operate at 10 MHz only if r_{mp} well exceeds 10^6. An interlamination insulation material with $r_{\text{mp}} \approx 10^7$ is required to fabricate the 95% fill-factor cores of which high-frequency performances are comparable to the 50% fill-factor counterparts with $r_{\text{mp}} \approx 10^6$.

E. Maximum Tolerable Conductivity of the Interlamination Insulation

Based on the analytical results, interlamination insulation is designed for the miniaturized laminated cores with $t_m = 2.2$ μm and a relatively small core width, $w = 0.5$ mm. Equation (41) can be utilized to calculate the exact $r_{\min,m}$, which is the lower bound of r_m. For the 50%-fill-factor cores operating at 10 MHz, the ratio $r_{\min,\text{mp}}$ is 5.18×10^4. Substituting the conductivity of permalloy and $r_{\min,\text{mp}}$ into (42) results in the maximum tolerable conductivity of the interlayer insulation ($\sigma_{\max,p}$) of 193 S/m. For the 95% fill-factor cores, $\sigma_{\max,p}$ is 10.2 S/m. These results imply that not only highly resistive oxide materials (e.g., SiO_2 and Al_2O_3), but also semiconducting materials with moderate conductivities, such as conducting oxides [23] and intrinsically conductive polymers [24], can be utilized as interlamination insulation materials at MHz frequencies. Note that the insulation thicknesses are dependent on the number of magnetic layers ($i+1$). As i increases, the insulation thicknesses (t_p) for 50% and 95% fill-factor cores will asymptotically approach 2.2 and 0.11 μm, respectively.

F. Theory Validation Using Finite Element Analysis

Finite element analysis (FEM)-based simulation is performed to validate the superposition assumption (i.e., $P_e = P_{e,i} + P_{e,d}$), which is central to the presented theoretical development. In particular, we compare the ratios of delocalized eddy current losses to intralayer eddy current losses ($P_{e,d}/P_{e,i}$), calculated based on two approaches: the theoretical calculation and the FEM simulation based on COMSOL. We model the abovementioned 50% fill-factor core which is designed for 10-MHz operation; the structural parameters are detailed in Fig. 6. The $P_{e,d}/P_{e,i}$ simulation is performed in two steps. First, the total eddy current losses, P_e, of the modeled laminated cores with various interlamination insulation conductivities (i.e., $\sigma_p = 0$, 1.93, 19.3, and 193 S/m) are calculated; note $\sigma_p = 193$ S/m is the maximum tolerable conductivity of the insulation for this laminated core, operating at 10 MHz. Since the laminated core with $\sigma_p = 0$ corresponds

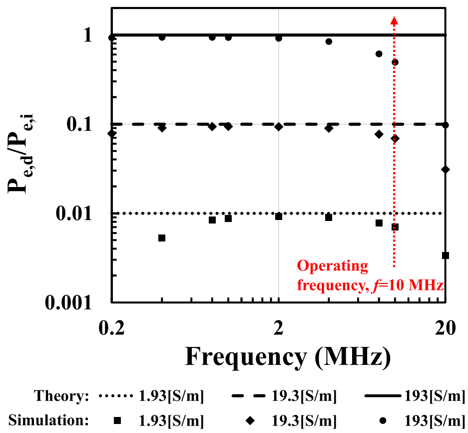

Fig. 6. Simulation and theoretical calculations of the ratio of delocalized eddy current losses to intralayer eddy current losses ($P_{e,d}/P_{e,i}$) as a function of frequency. The FEM was performed based on COMSOL 5.4a [core width (w) = 0.5 mm, number of magnetic layers ($i+1$) = 24, number of interlamination insulation layers (i) = 23, individual magnetic layer thickness/insulation layer thickness = 2.3 μm, and fill factor (γ) = 50%]. The conductivity of the interlamination insulation (σ_p) is varied from 1.93 to 193 S/m (i.e., maximum tolerable conductivity of the interlayer insulation, $\sigma_{\max,p}$).

to the discrete layer model, the calculated P_e with $\sigma_p = 0$ is the intralayer eddy current loss ($P_{e,i}$). Based on the superposition assumption, the delocalized loss ($P_{e.d}$) of the laminated core with a nonzero σ_p is calculated by subtracting $P_{e,i}$ (which is assumed independent of σ_p) from the corresponding P_e, simulated with respective σ_p. The ratios $P_{e,d}/P_{e,i}$ calculated from the simulation and the theoretical estimation [using (32)] are plotted as a function of frequency (see Fig. 6). The theoretical model corresponds relatively well to the simulated $P_{e,d}/P_{e,i}$ at various frequencies and interlamination insulation conductivities (σ_p) up to the operating frequency (10 MHz); the theoretical estimation of $P_{e,d}/P_{e,i}$ maxima is off by less than 10%. Note that the theory may significantly overestimate $P_{e,d}/P_{e,i}$ at extreme conditions. The discrepancies between the theoretical calculation and the simulation results are comparably larger when: 1) both $P_{e,d}/P_{e,i}$ and frequency are smaller (i.e., the lower left corner of Fig. 6) or 2) both $P_{e,d}/P_{e,i}$ and frequency are larger (i.e., the upper right corner of Fig. 6). The former error is attributed to small l (as small as 2) and very small eddy current losses at low frequencies that are comparable to FEM simulation errors, while the latter is attributed to large k (and/or k_m) which contradicts the demagnetization assumptions of the theory. Further details on the relationship between the error and the parameters l, k, and k_m may be found in the Appendix. The present theoretical analysis can assist a laminated core design process by enabling a simple, yet quantitative delocalized losses estimation, at desired high operating frequencies.

IV. Conclusion

The analytical studies of laminated core losses were extrapolated to elucidate the interlamination insulation design considerations of leaky laminated cores operating at high frequencies. The total eddy current loss from a laminated core with finite interlamination conductivities was assumed as the superposition of intralayer eddy current losses and delocalized losses. The higher bound of operating frequency, i.e., cutoff frequency, was defined at which the total eddy current losses begin to exceed the intrinsic hysteresis losses. By a systematic cutoff frequency analysis, the maximum tolerable conductivity of the interlayer insulation ($\sigma_{\max,p}$) was calculated, which characterizes the necessary quality of an interlamination insulation material.

An interlamination insulation was designed for a high-frequency (10 MHz) laminated core that could potentially process watts of power. We demonstrated that the insulations with moderate conductivity, ~1 S/m, is sufficient to suppress eddy currents within the cores even at the high frequency; Hence, in theory, electrodeposited laminated cores (which are fabricated based on a sequential electrodeposition of magnetic and semiconducting interlamination insulation materials as discussed in Section I) could be realized in which scalability, manufacturability, and superior high-frequency performance are combined. Further research on the realization and design optimization of such lamination solutions could foster the miniaturization of inductive components in many practical applications, including dc–dc switched-based converters.

Appendix

A. Verification of (1) and (3)

The resistance of the homogenized model along the y-axis (R_y) is

$$R_y = \rho_y \frac{T}{lw} = \rho_m \frac{\gamma T}{lw} + \rho_p \frac{(1-\gamma)T}{lw}. \tag{49}$$

Then

$$\rho_y = \rho_m \gamma + \rho_p (1-\gamma). \tag{50}$$

Similarly, the conductance of the model along the x-axis is

$$\frac{1}{R_x} = \sigma_x \frac{Tl}{w} = \sigma_m \frac{\gamma Tl}{w} + \sigma_p \frac{(1-\gamma)Tl}{w}. \tag{51}$$

Then

$$\sigma_x = \sigma_m \gamma + \sigma_p (1-\gamma). \tag{52}$$

Both (1) and (3) are accurate only if the following inequality is satisfied:

$$\begin{gathered} \rho_p(1-\gamma) \gg \rho_m \gamma \\ \frac{\rho_p}{\rho_p + \rho_m} \gg \gamma. \end{gathered} \tag{53}$$

If the maximum achievable fill factor is 95%

$$\frac{\rho_p}{\rho_p + \rho_m} \gg 0.95 \geq \gamma \tag{54}$$

or

$$\frac{\rho_m}{\rho_p} \ll \frac{1}{\gamma} - 1 = 0.053. \tag{55}$$

Hence, when $\rho_m/\rho_p \ll 0.001$, (or, in other words, $r_{\mathrm{mp}} = \sigma_m/\sigma_p \gg 1000$) and $\gamma \leq 0.95$, (1) and (3) are good approximations for σ_x and σ_y.

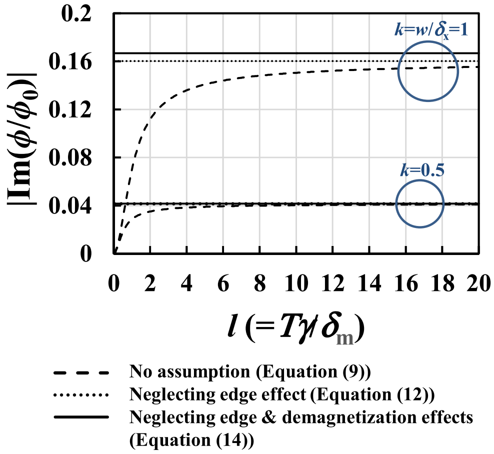

Fig. 7. Magnitude of the imaginary part of the normalized flux ($|\mathbf{Im}(\phi/\phi_0)|$) calculated based on three equations (9), (12), and (14).

B. Validation of Negligible End Effect and Negligible Demagnetization Assumptions

When the delocalized eddy currents are calculated, the end effect and the demagnetization within the core are neglected. Since the losses are in proportion to the magnitude of $\mathbf{Im}(\phi/\phi_0)$ as (15), it is important to quantify the differences between the magnitudes of $\mathbf{Im}(\phi/\phi_0)$ that are calculated from the rigorous solution (9), the solution which assumes negligible end effect (12), and the solution which assumes both negligible end effect and demagnetization (14). The calculations are presented in Fig. 7. Note that the rigorous solution (9) is a function of k and l, since it considers the boundary conditions from all four core edges, while other two, (12) and (14), are functions of k (not considering the top and bottom edges). We only consider $k \leq 1$, since $k > 1$ may correspond to $P_{e,d}/P_h$ larger than unity (see Fig. 3), which is out of the scope of this paper. Note that larger k will contradict the demagnetization assumption, and thus, increased error between the actual loss and the calculation will be observed [similarly, the intralayer eddy current losses cannot be accurately calculated using (23) when k_m is large]. The condition $l \geq 2$ should be considered, since the motivation of using a laminated core would be storing magnetic energy within a thick magnetic material of which total thickness ($T\gamma$) is at least larger than twice the skin depth of the material (t_m). As observed from Fig. 7, the magnitudes of $\mathbf{Im}(\phi/\phi_0)$ are overestimated as we add assumptions [in the worst case scenario, by $\sim$50% at $k = 1$ and $l = 2$, when comparing $\mathbf{Im}(\phi/\phi_0)$ calculated from (9) and (14)]. This discrepancy reduces as k decreases and/or l increases; the latter directly shows that the end effect from the top and bottom edges of a core can be neglected when the total thickness of the magnetic material is sufficiently large. Hence, the presented delocalized eddy current calculation based on the assumptions would be valid when designing practical laminated cores with large l. We also observed $\mathbf{Re}(\phi/\phi_0) > 0.968$ from (9) when $k \leq 1$ and $l \geq 2$; this also validates the demagnetization assumption behind (14). A similar analysis can be performed to validate the demagnetization assumption behind (20).

ACKNOWLEDGMENT

This work was carried out in part at the Singh Center for Nanotechnology, which is supported by the NSF National Nanotechnology Coordinated Infrastructure Program under Grant NNCI-1542153.

REFERENCES

[1] S. C. Mathuna, T. O'Donnell, N. Wang, and K. Rinne, "Magnetics on silicon: An enabling technology for power supply on chip," *IEEE Trans. Power Electron.*, vol. 20, no. 3, pp. 585–592, May 2005.

[2] C. R. Sullivan, D. V. Harburg, J. Qiu, C. G. Levey, and D. Yao, "Integrating magnetics for on-chip power: A perspective," *IEEE Trans. Power Electron.*, vol. 28, no. 9, pp. 4342–4353, Sep. 2013.

[3] C. Ó. Mathúna, N. Wang, S. Kulkarni, and S. Roy, "Review of integrated magnetics for power supply on chip (PwrSoC)," *IEEE Trans. Power Electron.*, vol. 27, no. 11, pp. 4799–4816, Nov. 2012.

[4] J. Kim *et al.*, "Nanolaminated permalloy core for high-flux, high-frequency ultracompact power conversion," *IEEE Trans. Power Electron.*, vol. 28, no. 9, pp. 4376–4383, Sep. 2013.

[5] D. Yao, C. G. Levey, R. Tian, and C. R. Sullivan, "Microfabricated V-groove power inductors using multilayer Co-Zr-O thin films for very-high-frequency DC-DC converters," *IEEE Trans. Power Electron.*, vol. 28, no. 9, pp. 4384–4394, Sep. 2013.

[6] R. Anthony, M. Hegarty, J. O'Brien, J. F. Rohan, and C. Ó. Mathúna, "Enhanced in-plane anisotropy and ferromagnetic resonance frequency in permalloy films laminated with nitrogen-doped tantalum," *IEEE Magn. Lett.*, vol. 8, 2017, Art. no. 5103304.

[7] M. Kim, J. Kim, F. Herrault, R. Schafer, and M. G. Allen, "A MEMS lamination technology based on sequential multilayer electrodeposition," *J. Micromech. Microeng.*, vol. 23, no. 9, 2013, Art. no. 095011.

[8] M. Kim, M. G. Allen, and J. Kim, "Nanolaminated CoNiFe cores with dip-coated fluoroacrylic polymer interlamination insulation: Fabrication, electrical characterization, and performance reliability," in *Proc. IEEE 67th Electron. Compon. Technol. Conf. (ECTC)*, Orlando, FL, USA, May/Jun. 2017, pp. 798–803.

[9] R. Anthony, Cian O'Mathúna, and J. F. Rohan, "MEMS based electrochemical process for fabrication of laminated micro-inductors on silicon," *Microelectron. Eng.*, vol. 155, pp. 33–38, Apr. 2016.

[10] L. V. Bewley and H. Poritsky, "Intersheet eddy-current loss in laminated cores," *Electr. Eng.*, vol. 56, no. 3, pp. 344–346, Mar. 1937.

[11] S. B. Shah, P. Rasilo, and A. Arkkio, "Eddy current loss calculation in burred laminated cores," in *Proc. IEEE Conf. Electromagn. Field Comput. (CEFC)*, Miami, FL, USA, Nov. 2016, p. 1.

[12] M. Veigel and M. Doppelbauer, "Analytic modelling of magnetic losses in laminated stator cores with consideration of interlamination eddy currents," in *Proc. Int. Conf. Elect. Mach. (ICEM)*, Sep. 2016, pp. 1339–1344.

[13] F. Bertoncini, E. Cardelli, S. D. Fraia, and B. Tellini, "Computing the surface impedance in nonlinear materials with hysteresis," *J. Appl. Phys.*, vol. 93, no. 10, pp. 6650–6652, 2003.

[14] J. Barranger, "Hysteresis and eddy-current losses of a transformer lamination viewed as an application of the poynting theorem," NASA, Washington, DC, USA, Tech. Rep. 3114, 1965.

[15] J. Lammeraner and M. Stafl, *Eddy Currents*. London, U.K.: Iliffe Books, 1966.

[16] K. Howard and M. K. Kazimierczuk, "Eddy-current power loss in laminated iron cores," in *Proc. IEEE Int. Symp. Circuits Syst.*, Sydney, NSW, Australia, vol. 3, May 2001, pp. 668–671.

[17] W. P. Taylor, M. Schneider, H. Baltes, and M. G. Allen, "A NiFeMo electroplating bath for micromachined structures," *Electrochem. Solid-State Lett.*, vol. 2, no. 12, pp. 624–626, 1999.

[18] J. Y. Park and M. G. Allen, "Development of magnetic materials and processing techniques applicable to integrated micromagnetic devices," *J. Micromech. Microeng.*, vol. 8, no. 4, p. 307, 1998.

[19] J. Kim, M. Kim, F. Herrault, J. Park, and M. G. Allen, "Highly laminated soft magnetic electroplated CoNiFe thick films," *IEEE Magn. Lett.*, vol. 4, 2013, Art. no. 5000204.

[20] R. Meere, T. O'Donnell, H. J. Bergveld, N. Wang, and S. C. O'Mathuna, "Analysis of microinductor performance in a 20-100 MHz DC/DC converter," *IEEE Trans. Power Electron.*, vol. 24, no. 9, pp. 2212–2218, Sep. 2009.

[21] (2017). *Soft Ferrite and Accessories Data Handbook*. [Online]. Available:https://www.ferroxcube.com/en-global/download/download/11

[22] H. Greve *et al.*, "Nanostructured magnetic Fe-Ni-Co/teflon multilayers for high-frequency applications in the gigahertz range," *Appl. Phys. Lett.*, vol. 89, no. 24, 2006, Art. no. 242501.

[23] T. Minami, “Present status of transparent conducting oxide thin-film development for Indium-Tin-Oxide (ITO) substitutes,” *Thin Solid Films*, vol. 516, no. 17, pp. 5822–5828, 2008.
[24] R. S. Kohlman *et al.*, “Limits for metallic conductivity in conducting polymers,” *Phys. Rev. Phys. Rev. Lett.*, vol. 78, no. 20, p. 3915, 1997.

Minsoo Kim received the B.S. and M.S. degrees in electrical and computer engineering from Seoul National University, Seoul, South Korea, in 2006 and 2008, respectively, and the Ph.D. degree from the Georgia Institute of Technology, Atlanta, GA, USA, in 2016.

Until 2009, he was with the Korea Institute of Industrial Technology, where he was involved in in inkjet-printed electronics. His current research interests include the development of electrodeposition-based technologies for the realization of micro/nanohierarchical structures that lead to a variety of useful applications, such as nanoscale magnetic laminations for miniaturized dc–dc converters, drag-reduced microfluidics, and nonlithographic nanopatterning.

Mark G. Allen (M’88–SM’04–F’11) received the B.A. degree in chemistry, the B.S.E. degree in chemical engineering, and the B.S.E. degree in electrical engineering from the University of Pennsylvania, Philadelphia, PA, USA, and the S.M. and Ph.D. degrees from the Massachusetts Institute of Technology, Cambridge, U.K.

In 1989, he joined the Faculty of the School of Electrical and Computer Engineering, Georgia Institute of Technology, Atlanta, GA, USA, ultimately holding the rank of Regents’ Professor and the J. M. Pettit Professorship in microelectronics, and a joint appointment in the School of Chemical and Biomolecular Engineering. In 2013, he left the Georgia Institute of Technology to become the Alfred Fitler Moore Professor of electrical and systems engineering and the Scientific Director of the Singh Nanotechnology Center, University of Pennsylvania. His current research interests include the development and the application of new micro- and nanofabrication technologies and MEMS.

Dr. Allen received the IEEE 2016 Daniel P. Noble Award for contributions to research and development, clinical translation, and commercialization of biomedical microsystems. He was the Editor-in-Chief of the *Journal of Micromechanics and Microengineering*, the Co-Chair of the IEEE/ASME MEMS Conference, and the Co-Founder of multiple MEMS companies, including Cardiomems and Axion Biosystems.